CRISPR-Cas9 gene editing and rapid detection of gene-edited mutants using high-resolution melting in the apple scab fungus, *Venturia inaequalis*

Mercedes Rocafort[1], Saadiah Arshed[2], Debbie Hudson[3], Jaspreet Singh[3], Joanna K. Bowen[2], Kim M. Plummer[4], Rosie E. Bradshaw[5,6], Richard D. Johnson[3], Linda J. Johnson[3] and Carl H. Mesarich[1,6,*]

[1]Laboratory of Molecular Plant Pathology, School of Agriculture and Environment, Massey University, Palmerston North 4410, New Zealand.

[2]The New Zealand Institute for Plant and Food Research Limited, Mount Albert Research Centre, Auckland 1025, New Zealand.

[3]Grasslands Research Centre, AgResearch Limited, Palmerston North 4410, New Zealand.

[4]Department of Animal, Plant and Soil Sciences, La Trobe University, AgriBio, Centre for AgriBiosciences, La Trobe University, Bundoora, Victoria 3086, Australia.

[5]Laboratory of Molecular Plant Pathology, School of Fundamental Sciences, Massey University, Palmerston North 4410, New Zealand.

[6]The New Zealand Bio-Protection Research Centre, Massey University, Palmerston North 4410, New Zealand.

[*]Corresponding author: Carl H. Mesarich: c.mesarich@massey.ac.nz

Abstract

Background: Scab, or black spot, caused by the filamentous fungal pathogen *Venturia inaequalis*, is the most economically important disease of apple (*Malus* x *domestica*) worldwide. To develop durable control strategies against this disease, a better understanding of the genetic mechanisms underlying the growth, reproduction, virulence and pathogenicity of *V. inaequalis* is required. A major bottleneck for the genetic characterization of *V. inaequalis* is the inability to easily delete or disrupt genes of interest using homologous recombination. Indeed, no gene deletions or disruptions in *V. inaequalis* have yet been published. Recently, CRISPR-Cas9 has emerged as an efficient tool for gene editing in filamentous fungi. With this in mind, we set out to establish CRISPR-Cas9 as a gene editing tool in *V. inaequalis*.

Results: We showed that CRISPR-Cas9 can be used for gene inactivation in the apple scab fungus. As a proof of concept, we targeted the melanin biosynthesis pathway gene *trihydroxynaphthalene reductase* (*THN*), which has previously been shown to result in a light-brown colony phenotype when transcriptionally silenced using RNA interference. Using one of two CRISPR-Cas9 single guide RNAs (sgRNAs) targeted to the *THN* gene, delivered by a single autonomously replicating Golden Gate-compatible plasmid, we were able to identify six of 36 stable transformants with a light-brown phenotype, indicating an ~16.7% gene inactivation efficiency. Notably, of these six *THN* mutants, five had an independent mutation. As part of our pipeline, we also report a high-resolution melting (HRM) curve protocol for the rapid detection of CRISPR-Cas9 gene-edited mutants of *V. inaequalis*. This protocol identified a single base pair deletion mutation in a sample containing only 5% mutant genomic DNA, indicating high sensitivity for mutant screening.

Conclusions: In establishing CRISPR-Cas9 as a tool for gene editing in *V. inaequalis*, we have provided a strong starting point for studies aiming to decipher the function of genes associated with the growth, reproduction, virulence and pathogenicity of this fungus. The associated HRM curve protocol will enable CRISPR-Cas9 transformants to be screened for gene inactivation in a high-throughput and low-cost manner, which will be particularly powerful in cases where the CRISPR-Cas9-mediated gene inactivation efficiency is low.

Keywords

CRISPR-Cas9, gene editing, *Venturia inaequalis*, apple scab, apple black spot, high-resolution melting (HRM) curve analysis, *trihydroxynaphthalene reductase* (*THN*) gene, melanin biosynthesis pathway disruption.

Introduction

Fungal species from the *Venturia* genus are devastating plant pathogens of economically important crops that mainly belong to the *Rosaceae* (1-3). The best researched of these pathogens is *Venturia inaequalis*, which causes scab, or black spot, the most economically important disease of apple (*Malus* x *domestica*) worldwide (1). Under favourable conditions, this disease can result in 70% or more of the crop being lost, as scab renders the apples unmarketable (i.e. through blemishes and deformation), and reduces both the growth and yield of the plant (i.e. by causing repeated defoliation of trees over several seasons) (1, 3, 4). To develop durable control strategies against scab disease, a better understanding of the

69 genetic mechanisms underlying the growth, reproduction, virulence and pathogenicity of
70 *V. inaequalis* is required.

71 A key development over recent years has been the availability of several *V. inaequalis*
72 genome sequences and gene catalogues (2, 5-9), as well as the development of both
73 polyethylene glycol (PEG)-mediated protoplast and *Agrobacterium tumefaciens*-mediated
74 transformation protocols for use with this fungus (10). However, while several *V. inaequalis*
75 genes of interest that are putatively involved in the infection process of apple have been
76 identified (5, 11-15), none have been functionally characterized to date using traditional gene
77 deletion or disruption techniques. Indeed, no gene deletions or disruptions, based on
78 homologous recombination, have yet been reported for *V. inaequalis* in the literature. This
79 suggests that gene deletion or disruption by traditional homologous recombination is
80 extremely inefficient in *V. inaequalis*. It should be noted that transcriptional silencing of
81 multiple genes in *V. inaequalis* has been achieved using RNA interference (RNAi) (16).
82 However, RNAi does not typically silence a gene to completion and the observed phenotypes
83 can be inconsistent, unclear or absent, making it difficult to determine function (17, 18).
84 Taken together, alternative gene disruption and deletion tools, such as the Clustered
85 Regularly Interspaced Short Palindromic Repeats-Cas9 (CRISPR-Cas9) system (19), are
86 desperately needed to assess gene function in *V. inaequalis*.

87 The CRISPR-Cas9 system is a powerful tool for gene editing that has been established
88 in many species of filamentous plant-pathogenic microbes. Indeed, CRISPR-Cas9 has been
89 used to generate gene inactivations in more than 40 species of filamentous fungi and
90 oomycetes (20), including *Phytophthora sojae* (21), *Magnaporthe oryzae* (22), *Ustilago*
91 *maydis* (23) and a fungus that is closely related to *V. inaequalis*, *Leptosphaeria maculans* (24).

The CRISPR-Cas9 gene editing system requires two components: the Cas9 endonuclease and a single guide RNA (sgRNA). The Cas9 endonuclease is an RNA-guided enzyme that generates a double strand break (DSB) in the genome. The sgRNA consists of a protospacer sequence of 20 nucleotides at the 5' end that targets specific DNA by base pairing, and an 80-nucleotide scaffold structure that binds to Cas9. The sgRNA-Cas9 complex only cleaves the target DNA if it is flanked by a protospacer motif (PAM) (19).

After the Cas9 endonuclease generates a DSB in the target DNA, DNA repair mechanisms are activated (19, 25). The DNA can be repaired by a non-homologous end-joining mechanism (NHEJ) or homology-directed repair (HDR), although NHEJ is usually the dominant DNA repair pathway in fungi (26). DNA repair by NHEJ is error-prone and is likely to introduce small insertions/deletions (indels) or nucleotide substitutions, which can lead to frameshift mutations that cause a gene disruption (25). Alternatively, a double-stranded DNA template (donor DNA), usually harbouring a selectable marker, can be introduced to use as a repair template for HDR.

Traditionally, screening for the identification of mutants generated by the CRISPR-Cas9 system can be achieved using an enzymatic mismatch cleavage (EMC) method (27) or a polyacrylamide gel electrophoresis (PAGE)-based method (28) that both rely on the detection of DNA heteroduplexes. Both EMC and PAGE detect large indels with a similar efficiency; however, the sensitivity with which they detect small indels (i.e. the type of indels that are usually generated by CRISPR-Cas9 DSB) is low (27-29)**.** Alternatively, CRISPR-Cas9 mutants can be identified by amplicon sequencing, which is a tedious and expensive process. High-resolution melting (HRM) curve analysis is a fluorescence-based technique that measures the melting temperature of double- stranded DNA and, in doing so, can discriminate between

115 amplicons with different melting temperatures (30-32). HRM curve analysis has been widely
116 used to identify mutations and single nucleotide polymorphisms in various genes (30, 33), and
117 has recently been used to reliably identify CRISPR-Cas9-mediated base pair (bp) indels in
118 plants (29, 34). To date, even though HRM curve analyses are largely used for fungal species
119 identification, to our knowledge, an HRM curve analysis has not yet been employed to screen
120 for CRISPR-Cas9-generated mutants in fungi.

121 In this study, we set out to establish the CRISPR-Cas9 gene editing system in
122 *V. inaequalis*. For this purpose, we first generated the Golden Gate-compatible plasmid
123 Cas9HygAMAccdB by modifying the previously published Cas9 autonomously replicating
124 plasmid ANEp8_Cas9_LIC1 (35). Here, Golden Gate-compatibility was chosen as it enabled the
125 introduction of a sgRNA into Cas9HygAMAccdB using a single step, facilitating the creation of
126 a Cas9HygAMA-*sgRNA* plasmid in less than one week. Next, using the melanin biosynthesis
127 pathway gene *trihydroxynaphthalene reductase* (*THN*) as a proof of concept, we showed, in
128 conjunction with the Cas9HygAMA-*sgRNA* plasmid, that the CRISPR-Cas9 gene editing system
129 can be successfully applied to *V. inaequalis*. As part of this process, we also established a
130 method based on an HRM curve analysis for the high-throughput screening of CRISPR-Cas9
131 gene-edited mutants of *V. inaequalis*.

132

133 **Results and discussion**

134 **CRISPR-Cas9 can be used for gene disruption in *V. inaequalis***

135 We set out to establish the CRISPR-Cas9 gene editing system in *V. inaequalis*, using the
136 melanin biosynthesis pathway gene *THN* (Joint Genome Institute ID: *atg4736.t1*) as a target

for inactivation. The *THN* gene was chosen as a proof of concept, as a previous study had shown that *V. inaequalis* displays a distinctive light-brown phenotype when this gene is transcriptionally silenced using RNAi, indicative of reduced melanisation (16). In this way, transformants of *V. inaequalis* inactivated for the *THN* gene using the CRISPR-Cas9 gene editing system can be rapidly identified through a simple visual screen. For ease of use, we chose to employ a CRISPR-Cas9 gene editing system that, similar to the one previously established in *Aspergillus niger* (35), only requires a single autonomously replicating plasmid, Cas9HygAMAccdB (containing both the Cas9 endonuclease and sgRNA), for gene inactivation.

The Cas9HygAMAccdB plasmid contains an *A. niger* codon-optimized *cas9* gene expressed under the control of the *pkiA* (*pyruvate kinase*) promoter. To ensure expression in the fungal nucleus, the Cas9 endonuclease was tagged at its carboxyl (C) terminus with a nuclear localization signal (NLS). The Cas9HygAMAccdB plasmid also contains an RNA polymerase III promoter to facilitate expression of the sgRNA *in vivo.* Using the chosen CRISPR-Cas9 system, the 20 nucleotides of the sgRNA protospacer were synthesized as two pairs of complementary oligonucleotides that were pre-annealed and cloned into Cas9HygAMAccdB by a single-step Golden Gate reaction, enabling Polymerase Chain Reaction (PCR)-free cloning that could be completed in less than one week.

An autonomously replicating plasmid was chosen as it has several advantages. Firstly, autonomously replicating plasmids can enhance fungal transformation efficiency, as recombination between the plasmid and chromosome is not required (36). As such, autonomously replicating plasmids can be used in fungal species that exhibit low transformation efficiency, such as *V. inaequalis*. Secondly, autonomously replicating plasmids could be lost once selection (e.g., as mediated through hygromycin B) is removed (36). In

doing so, autonomously replicating plasmids can reduce off-target effects by only enabling transient expression of the Cas9 endonuclease in the fungus (37). As such, autonomously replicating plasmids could be recycled, which would enable the sequential inactivation of genes in CRISPR-Cas9 gene-edited mutants and could also facilitate the subsequent complementation of mutants generated using CRISPR-Cas9 technology.

As a starting point for inactivation, sgRNAs were designed to target the amino (N) terminus (first and second exon) instead of the C terminus of the *THN* gene. This is because mutations at the C terminus of a gene are less likely to cause a frameshift mutation that results in inactivation (38). As different sgRNAs can display different targeting efficiencies (38), two different sgRNAs, sgRNA 4 and sgRNA 20, with similar predicted on-target activity, and no predicted off-target activity (Table 1), were selected for inactivation of the *THN* gene. Special attention was taken to ensure that the sgRNAs did not target any other melanin biosynthesis pathway genes that have a high degree of conservation to *THN*, such as the *1,3,6,8-tetrahydroxynaphthalene reductase* gene (Joint Genome Institute ID: *atg3631.t1*). PEG-mediated protoplast transformation of *V. inaequalis* with sgRNA 4, targeting the first *THN* exon (Figure 1.A), resulted in 98 independent transformants, of which 62 ceased to grow on hygromycin B selection media after one week, and were therefore considered transient, giving a final number of 36 stable transformants. Transient transformants have been reported in a large number of PEG-mediated protoplast transformations of fungi (39, 40), and it has previously been reported that up to 98% of PEG-mediated protoplast transformants of *V. inaequalis* are transient (10). Of course, it remains possible that the large number of transient transformants generated in our study was the result of premature loss of the autonomously replicating plasmid used to deliver the sgRNA and Cas9.

Notably, of the 36 stable transformants, six had a light-brown phenotype (Figure 1.B). These were transformants THN #9, THN #37, THN #60, THN #66, THN #89 and THN #96. To validate the presence of a mutation in the *THN* gene, it was amplified from each of the six putative mutants by PCR, as well as from three dark-brown transformants without the light-brown phenotype (THN #38, THN #53 and THN #90), and subjected to amplicon sequencing. As expected, all three dark-brown transformants did not contain a mutation in their *THN* gene (Figure 1.C). For the putative light-brown mutant THN #9, the *THN* gene could not be amplified by PCR using two different sets of primers (MR161-MR162, MR185-MR186). This was despite the fact that both *THN*-flanking genes could be amplified, suggesting that a large deletion at the *THN* locus might have occurred (Figure S1). In contrast to the dark-brown transformants, the remaining light-brown *THN* transformants displayed a range of mutations. More specifically, these were a single bp insertion (T) at the same location in THN #37 and THN #66, a 33-bp deletion (TTTGGAGGGCAAGGTCGCCCTCGTTACCGGTTC) in THN #60, a single bp deletion (T) in THN #89, and a 24-bp deletion (TCATGGTCTTTGGAGGGCAAGGTC) in THN #96. Therefore, from the 36 stable transformants, six had a confirmed mutation, giving a gene inactivation efficiency of ~16.7%.

CRISPR-Cas9 gene inactivation efficiencies in other filamentous fungi, in experiments that rely on NHEJ, range between 10 and 100% (22, 23, 41-43). In cases where the CRISPR-Cas9 NHEJ-based gene inactivation efficiency is low, the gene inactivation efficiency could be improved greatly by the incorporation of a donor DNA that is integrated into the genome using HDR (22). Nevertheless, gene inactivation efficiencies between experiments cannot be compared, as these efficiencies will greatly depend on Cas9 expression, sgRNA design and accessibility of the target gene, among other factors (20). Therefore, even though the inactivation efficiency of the *V. inaequalis THN* gene with sgRNA 4 is at the low end, it is likely

to vary between genes and no conclusions can yet be drawn as to the overall efficiency of the technique.

Remarkably, PEG-mediated protoplast transformation of *V. inaequalis* with sgRNA 20, targeting the second exon of the *THN* gene (Figure 1.A), resulted in a similar number of stable independent transformants on hygromycin B selection media (31 in total), but none of these transformants had the distinctive light-brown phenotype. This stark difference in the number of transformants inactivated for the *THN* gene is interesting, given that both sgRNAs had a similar predicted on-target activity score (Table 1). However, different sgRNAs can vary greatly in efficiency, as with that previously observed for the *yA* gene of the filamentous fungus *A. nidulans* (44), highlighting the importance of reliable methods to estimate sgRNA efficiency. Thus, while genes will differ in their ability to be inactivated using the CRISPR-Cas9 gene editing system (e.g. due to their location in the genome) (20), it is important that future studies consider multiple sgRNAs for successful gene inactivation in *V. inaequalis*.

Table 1: Selected sgRNA protospacers used to target the *Venturia inaequalis* melanin biosynthesis pathway gene *trihydroxynaphthalene reductase* (*THN*).

	Sequence (5'–3')[1]	**Binding site**	**Direction**	**Off-targets[2]**	**Off-target score[3]**	**On-target score[4]**
Protospacer 4	GCCCCATCATGGTCTTTGGAGGG	Exon 1	Forward	0 (0 in CDS)	100%	0.448
Protospacer 20	TTTCAAGGACGTCACACCAGAGG	Exon 2	Forward	0 (0 in CDS)	100%	0.539

[1]NGG: protospacer adjacent motif (PAM) site.
[2]CDS: coding sequence.
[3]Off-target score: prediction of how likely a sgRNA sequence might bind to somewhere else in the genome. Scores are between 0 and 100, with higher scores indicative of less off-target activity.
[4]On-target scores are between 0 and 1, with higher scores indicative of higher expected activity of the sgRNA-Cas9 complex on the target gene, based on (38).

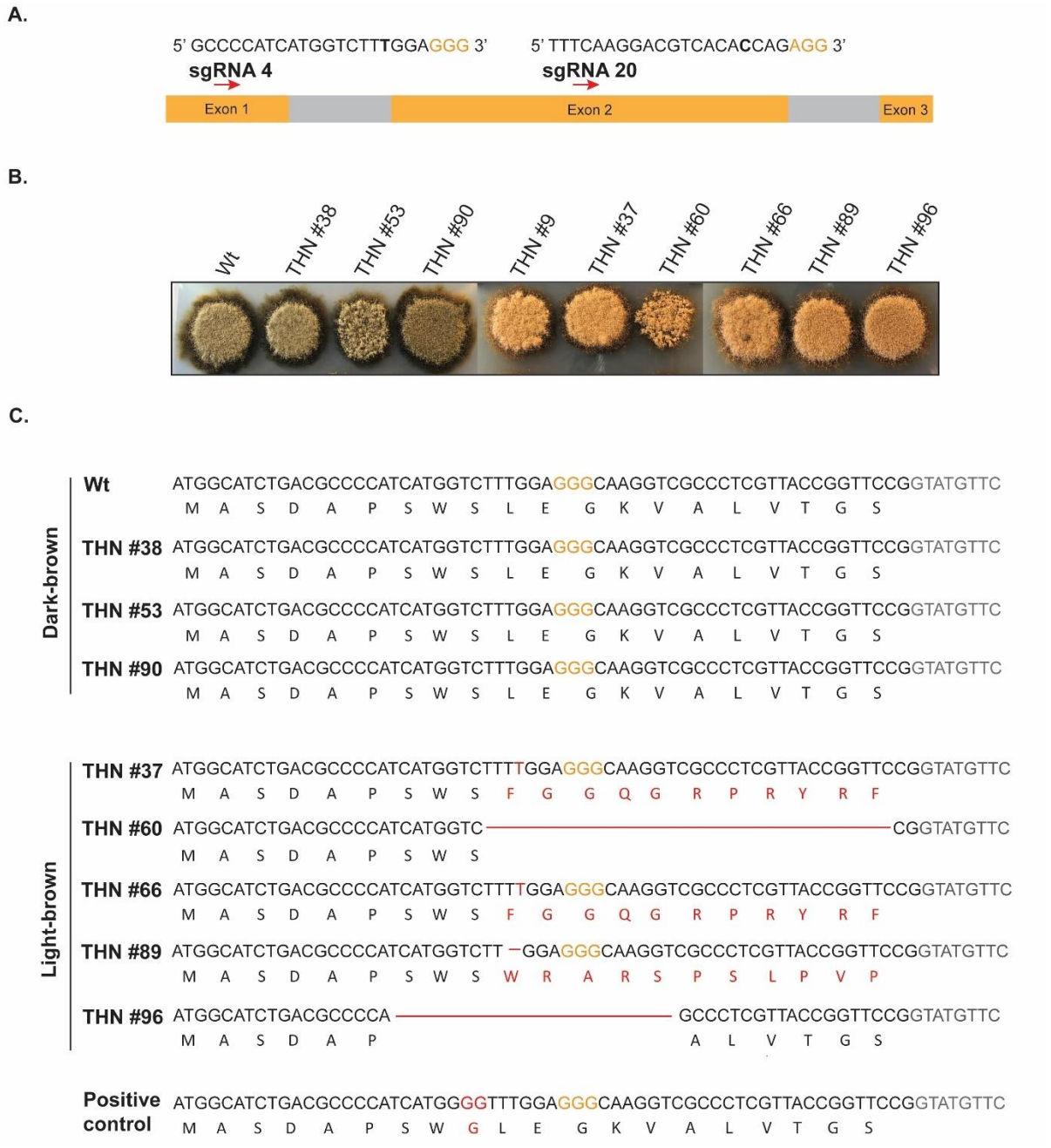

Figure 1. Establishment of the CRISPR-Cas9 gene editing system in *Venturia inaequalis*. A. Schematic representation of the *V. inaequalis* melanin biosynthesis pathway gene *trihydroxynaphthalene reductase* (*THN*; 911 bp) with binding sites for the two selected sgRNAs used in CRISPR-Cas9 gene editing experiments shown. Orange: gene exons; Grey: gene introns; Bold nucleotides: expected sgRNA cleavage site; orange nucleotides: PAM site. Arrows: binding direction of sgRNAs. **B.** Colony phenotype of wild type (wt) *V. inaequalis*, and three dark-brown and six light-brown CRISPR-Cas9 transformants grown on potato-dextrose agar at 22°C for 14 days. **C.** Spectrum of CRISPR-Cas9-generated mutations in the *THN* gene. Black nucleotides: exon; Grey nucleotides: intron; Orange nucleotides: PAM site; Red amino acids/nucleotides: mutations observed. Light-brown mutant THN #9 was not sequenced due to a lack of PCR amplification for the *THN* gene.

The autonomously replicating CRISPR-Cas9 gene editing plasmid is rapidly lost in most transformants once selection is removed

With the finding that the CRISPR-Cas9 gene editing system could be successfully applied to *V. inaequalis*, we next set out to determine whether this fungus can lose the autonomously replicating plasmid, Cas9HygAMA-*sgRNA*, once the hygromycin B selection is removed. For this purpose, all six light-brown *THN* mutants (THN #9, THN #37, THN #60, THN #66, THN #89 and THN #96), as well as three dark-brown transformants (THN #38, THN #53 and THN #90), all derived from the transformation of *V. inaequalis* with sgRNA 4, were single-spore purified and replica-plated onto both potato-dextrose agar (PDA) and PDA supplemented with 50 µg/ml hygromycin B. After only one round of single-spore isolation and sub-culturing, four of the *THN* mutants (THN #60, THN #66, THN #89 and THN #96) and two of the transformants without the light-brown phenotype (THN #53 and THN #90) lost the Cas9HygAMA-*sgRNA* plasmid and were therefore unable to grow on PDA supplemented with hygromycin B, indicating loss of the Cas9HygAMA-*sgRNA* plasmid (Figure S2).

High-resolution melting analysis is a sensitive and high-throughput method to screen for CRISPR-Cas9 mutants

In our study, mutants of *V. inaequalis* with a CRISPR-Cas9-mediated gene inactivation of the *THN* gene could be rapidly identified based on their light-brown colony phenotype. However, not all genes of *V. inaequalis* will result in an observable phenotype when inactivated or mutated. For this reason, a low-cost, high-throughput method is required to rapidly identify CRISPR-Cas9 gene-edited mutants of *V. inaequalis* that lack an observable phenotype on a

transformation plate facilitating selection. One such method is an HRM curve analysis, which enables the rapid identification of single bp indels in DNA amplicons from transformant genomic DNA (30-32). We set out to test the efficiency of an HRM curve analysis for the detection of *V. inaequalis THN* mutants generated using CRISPR-Cas9 sgRNA 4. As a starting point for this analysis, we first generated a positive control sequence for detecting indels relative to the wild type (wt) sequence (Figure 1.C). The positive control was generated by introducing a two-nucleotide substitution into a PCR amplicon of the *THN* gene using site-directed mutagenesis.

According to the literature, an HRM curve analysis can be affected by different parameters such as genomic DNA quality, PCR amplicon size, amplicon GC content and fluorescent dye used (45). To ensure reliability of the assay, good quality genomic DNA should be extracted. Likewise, the same DNA preparation method should be used across all samples to ensure uniformity in genomic DNA quality. Amplicon size is another crucial parameter that affects the HRM curve analysis. Therefore, two different primer sets were designed to generate amplicons of 230 bp (MR170-MR171) and 123 bp (MR172-MR173) (Table 2). The HRM curve assay was performed with both primers sets using wt genomic DNA and the engineered positive control as DNA template. Specific DNA amplicons could be amplified using both primers sets (Figure 2.A); however, the smaller amplicon showed a clearer shift in the melting curve between wt and positive control (Figure 2.B). Given that smaller amplicons are more suitable for HRM curve analysis (45), and because the smaller amplicon showed a clearer shift in the melting curve, we decided to use the 123 bp amplicon for our screen (primer set MR172-MR173).

Table 2. Oligonucleotides used in this study. Bold sequence corresponds to the *Sap*I restriction site. Italicised sequence corresponds to the *Not*I restriction site. Bold italicized sequence corresponds to the *Kpn*I restriction site.

Oligonucleotide name	Oligonucleotide sequence (5´–3´)
MR135	**GTC**TTTCAAGGACGTCACACCAG
MR136	**AAC**CTGGTGTGACGTCCTTGAAA
MR137	**GTC**GCCCCATCATGGTCTTTGGA
MR138	**AAC**TCCAAAGACCATGATGGGGC
MR139	TTTTCTCTTCCATTTACGC
MR161	GTAGGGAGGTCCATTAGTG
MR162	GGATAACACACTAGAGATA
MR170	TTATAGTCGACCACCGCTCG
MR171	CCACGACCTGTTGATTGCAT
MR172	CCCACTCACTAAACAAACTA
MR173	TCGATTGACAAGAACATACC
MR182	GCATCTGACGCCCCATCATGGGGTTT
MR183	AAACCCCATGATGGGGCGTCAGATGC
MR184	GCGAGAATGCAGAGAGTTGG
MR185	GTGTGTGTCGCTGGATGATC
MR204	CGCCAGCCTTCAATGCCAAT
MR205	CATTGCGCCATCCCGATCTG
MR252	CGTTGGCCAATCAGACGTCG
MR253	GCCCAGAGCATCATCACCCT
KpnI TtrpC Hyg DONR R	GCC***GGTACC***GCGCTTACACAGTACACGAG
NotI PgpdA Hyg pDONR F	AAGGAAAAAA*GCGGCCGC*CTAAAATCCGCCGCCTCCAC
SapI site CRISPR Fw P1	GTCGGAAGAGCAAAAT**GCTCTTC**AGTTTTAGAGCTAGAAATAGCAAG
SapI site CRISPR Rev P1	AACTGAAGAGCATTTT**GCTCTTC**CGACGAGCTTACTCGTTTCG
Fw LIC2	CAACCTCCAATCCAATTTGACTCCGCCGAACGTACTGG
Rev LIC2	ACTACTCTACCACTATTTGAAAAGCAAAAAAGGAAGGTACAAAAAAGC
SapI ccdB F	TCGGCTCGTCGGAAGAGCGACCGACAGCCTTCCAAATG
SapI ccdB R	TCGCTAAAACTGAAGAGCGTTGGCAGCATCACCCGACG

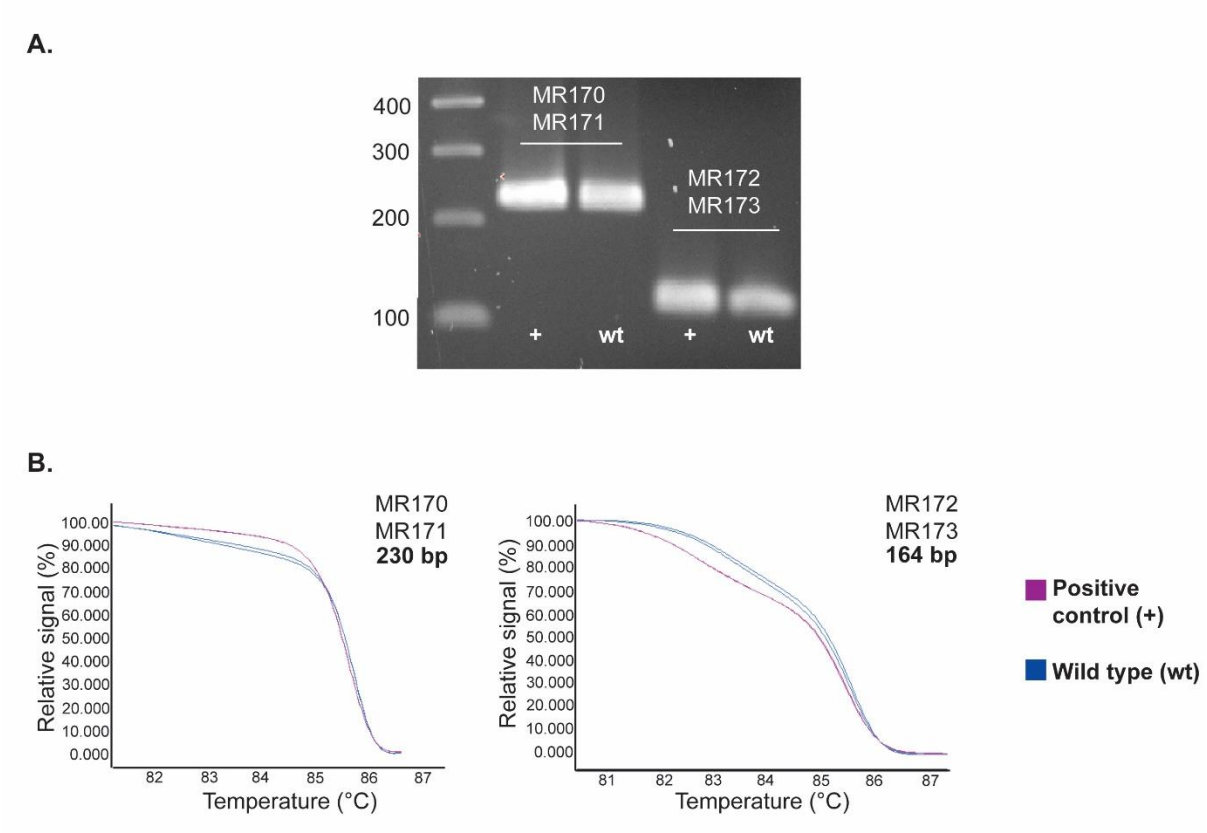

Figure 2. Optimization of primers for qPCR-HRM curve analysis of the *trihydroxynaphthalene reductase* (*THN*) gene mutants generated using CRISPR-Cas9 sgRNA 4. A. Conventional PCR amplification of the *THN* gene positive control (+) and wild type (wt) sequences with the different primer sets resolved by electrophoresis on a 1.5% TBE agarose gel. Ladder sizes are shown in base pairs (bp). **B.** Normalized and shifted melting curves of the *THN* gene positive control (+) and wild type (wt) PCR amplicons generated with two different primer sets (MR170-MR171 and MR172-MR173).

Initially, the Bioline SensiFAST™ SYBR® No-ROX Kit fluorescent dye was tested to perform the HRM curve analysis; however, no differences between the wt and engineered positive control DNA could be detected (data not shown). It is known that the fluorescent dye used for an HRM curve analysis is crucial to ensure good assay sensitivity, and that high-saturating dyes designed to increase sensitivity are commercially available. With this in mind, the HRM was repeated using the AccuMelt HRM SuperMix high saturating dye SYTO 9™, resulting in clear separation of unique melting curves between mutants (Figure 3). The normalized HRM curves showed that amplicons from wt fungus, as well as dark-brown

transformants, clustered together into a group with a similar melting curve profile (blue curves in Figure 3). In contrast, amplicons from the engineered positive control (green curves in Figure 3) and the light-brown *THN* mutants showed distinct melting curves (green, red, grey and purple curves in Figure 3) that correlated with the different mutations seen in Figure 1.C. These results indicate that the HRM curve assay can not only efficiently identify CRISPR-Cas9 gene-edited mutants, but can also discriminate between different mutations. The light-brown mutant THN #9 could not be screened using the HRM curve analysis due to a lack of PCR amplification for the *THN* gene, suggesting that a large deletion at the *THN* locus has been generated. This highlights one of the main limitations of the HRM curve analysis, in that it is not suitable for the detection of large deletion mutants. However, given that such deletion mutants can be easily assessed using standard PCR, this is not an issue.

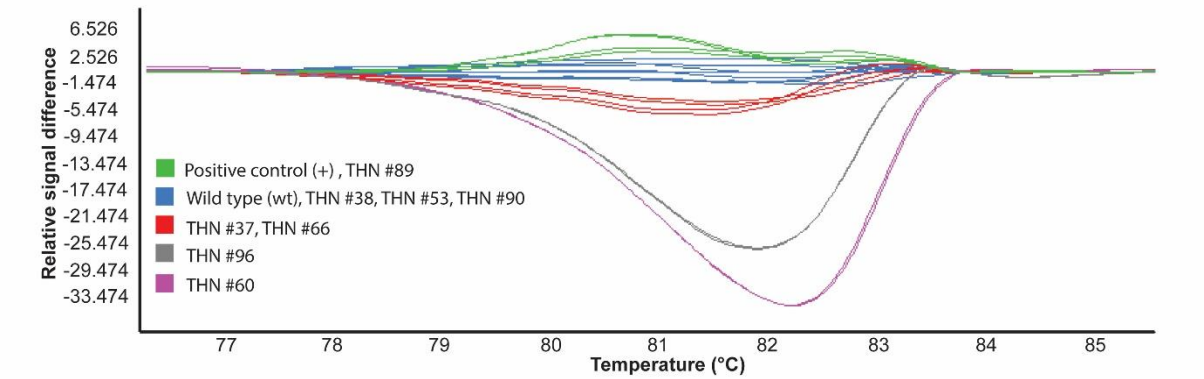

Figure 3. Screening of CRISPR-Cas9 transformants of *Venturia inaequalis* using qPCR-HRM curve and PCR amplicon sequencing analyses. Plot showing normalized and temperature-shifted differences in melting curves between *trihydroxynaphthalene reductase* (*THN*) amplicons of transformants. Melting curve groups were generated by LightCycler® 480 gene scanning software with a sensitivity of 0.40 and using AccuMelt HRM SuperMix fluorescent dye (DNAture). The experiment is based on two technical replicates per sample.

One of the main advantages of the HRM curve analysis is that it can detect mutant DNA that is mixed in with wt DNA, even when the amount of mutant DNA is as low as 1–5% (29, 34). To test the efficiency of the HRM curve assay, genomic DNA from one mutant with a

single bp insertion (THN #66) was mixed with wt genomic DNA at different mutant:wt ratios (1:99, 5:95, 10:90, 20:80, 30:70 and 50:50), similarly to that performed by (29). Under our conditions, the assay could not differentiate mutant and wt in 1:99 mutant:wt ratio; however, the mutant DNA could be identified by the HRM curve analysis in all of the other ratios, with a clear shift in the melting curve, indicating an assay sensitivity as high as 5% (Figure 4). Therefore, mutants do not need to be single-spore purified before performing an HRM curve analysis, and multiple mutants can be pooled together for large-scale screens. The observation that mutant DNA can be detected when mixed with wt DNA further reduces the cost and workload of the assay, and further validates the use of an HRM curve analysis for the high throughput screening of CRISPR-Cas9 fungal transformants.

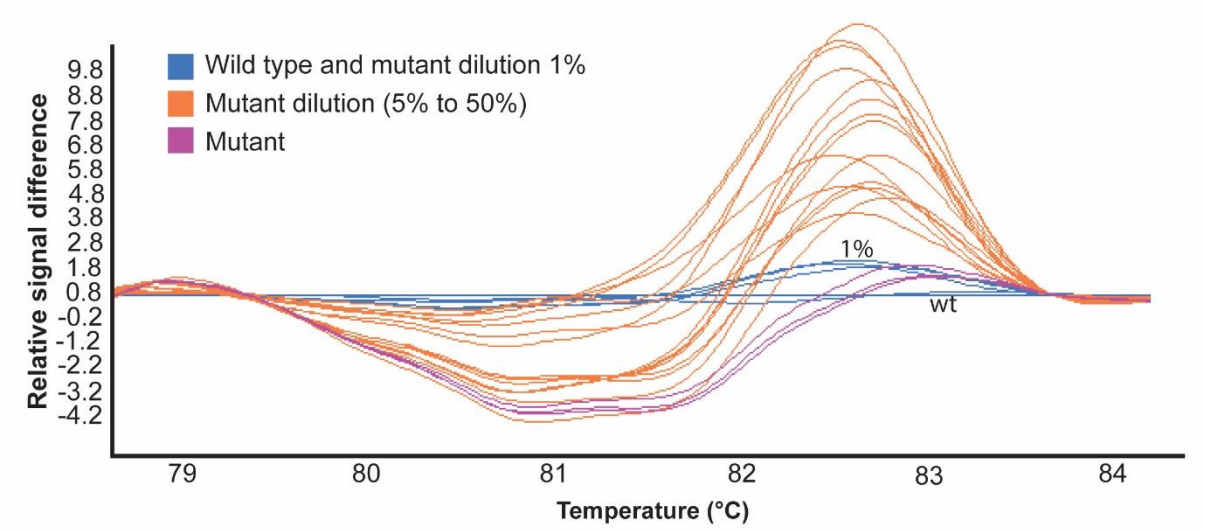

Figure 4. qPCR-HRM sensitivity to detect a one base pair deletion in mutant–wild type DNA mixtures. Plot showing normalized and temperature-shifted differences in melting curves between wild type (wt) *trihydroxynaphthalene reductase* (*THN*) DNA samples of *V. inaequalis* wt mixed with mutant *THN* DNA samples to detect the resolution limit of the HRM curve assay. Melting curve groups generated by LightCycler® 480 gene scanning software with a sensitivity of 0.48 and using AccuMelt HRM SuperMix fluorescent dye (DNAture). A minimum of two technical replicates were performed per sample. Wt genomic DNA and mutant THN #66 genomic DNA were diluted in different ratios (mutant:wt): 1:99, 5:95, 10:90, 20:80, 30:70 and 50:50.

353 **CRISPR-Cas9 editing of the *THN* gene does not alter the phenotype of *V. inaequalis* grown**
354 **in culture**

355 CRISPR-Cas9-based experiments can sometimes be detrimental to the target organism due to
356 Cas9 toxicity and/or off-target mutations (46), even though CRISPR-Cas9 off-target mutations
357 have been reported to be unlikely in different filamentous fungi (22, 23, 47). To test if CRISPR-
358 Cas9-mediated transformation has greatly affected the phenotype of *V. inaequalis* (e.g.
359 through toxicity or off-target effects), we investigated the phenotypes of the wt, three dark-
360 brown transformants (THN #38, THN #53, THN #90) and six light-brown mutants (THN #9,
361 THN#37, THN#60, THN#66, THN#89, THN#96) of *V. inaequalis* on and in cellophane
362 membranes overlaying PDA. During growth in cellophane membranes, *V. inaequalis*
363 undergoes morphological differentiation, similar to that observed under the cuticle *in planta*,
364 where it develops infection structures called runner hyphae and stromata (12). Therefore, we
365 investigated whether the *THN* mutants maintained their ability to develop runner hyphae and
366 stromata in cellophane membranes after CRISPR-Cas9-mediated transformation (Figure 5).
367 All mutants showed a similar phenotype to wt, in that they were able to penetrate the
368 cellophane membrane to develop runner hyphae and stromata. Likewise, all mutants
369 maintained their ability to sporulate on the cellophane membrane surface. Taken together,
370 these results suggest that CRISPR-Cas9-mediated transformation has not greatly affected the
371 phenotype of *V. inaequalis*. A more in-depth analysis based on whole genome sequencing is
372 the next step to determine whether this experiment has resulted in any off-target mutations.

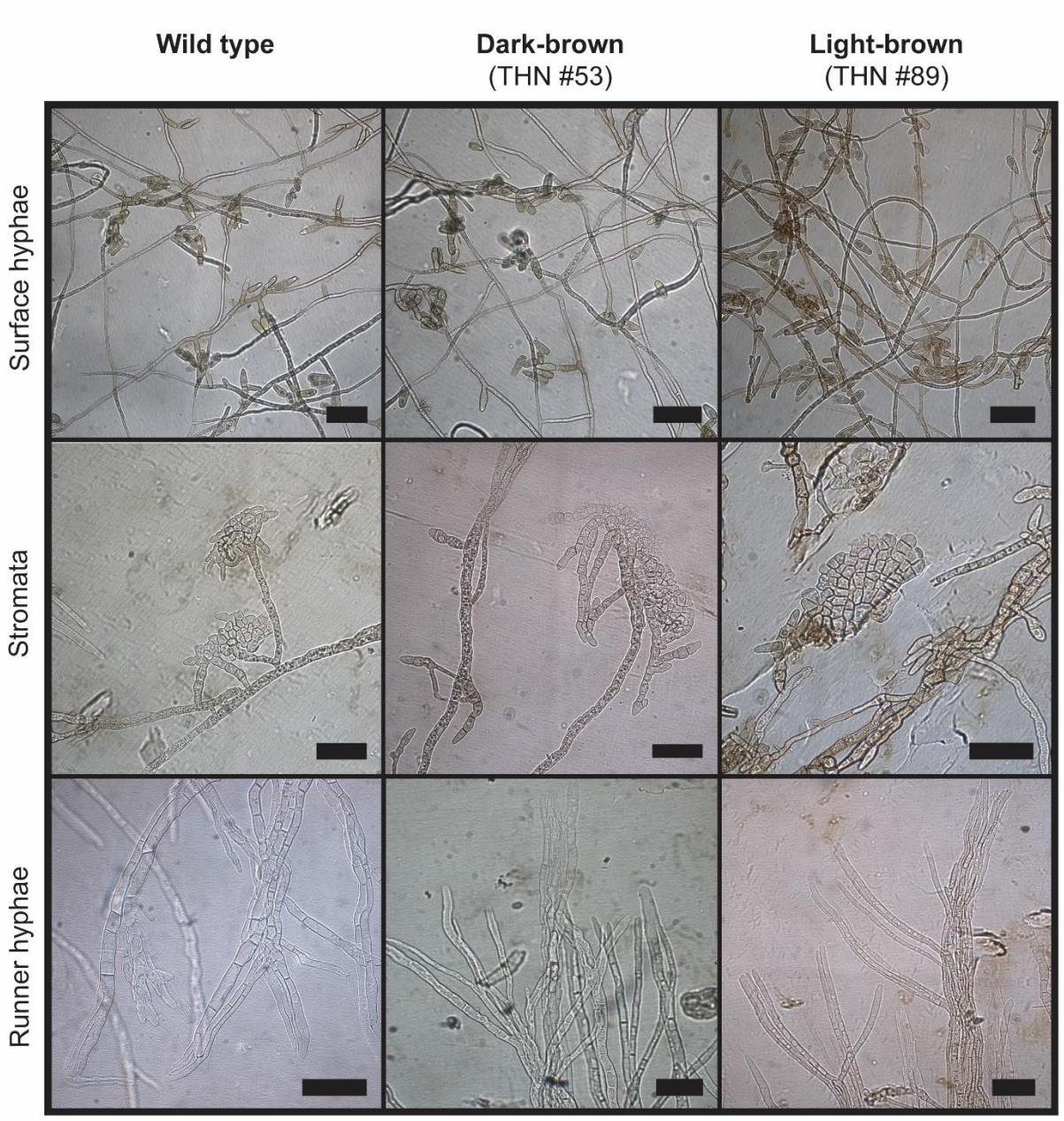

373

374 **Figure 5. In-culture phenotype of wild-type and CRISPR-Cas9 transformants of *Venturia***
375 ***inaequalis* on and in a cellophane membrane.** The conidia of each strain were plated on a
376 cellophane membrane overlaying potato-dextrose agar, followed by incubation at 22°C for
377 10 days. Scale bar 50 µM. Pictures are representative of all *THN* mutants identified.

378

379 **Conclusions**

380 We have successfully applied CRISPR-Cas9 gene editing to the filamentous fungal pathogen,

381 *V. inaequalis*, providing an opportunity for future studies to characterise gene functions

associated with the growth, reproduction, virulence and pathogenicity of this fungus. Given that the genomes of several other species from the *Venturia* genus have recently been sequenced (5, 48-53), this development will likely be useful for the functional characterization of genes in these species. Notably, genome sequencing has revealed that members of the *Venturia* genus contain large expanded families of putative effector genes that likely play an important role in host colonization (5). As the functional characterization of gene families is often hindered by functional redundancy between family members, and because the sequential deletion of family members using standard homologous recombination is limited by the number of selectable marker genes that are available, our finding that CRISPR-Cas9 technology can be applied to *V. inaequalis* is also expected to greatly facilitate the functional characterization of effector gene families in the *Venturia* genus (i.e. through sequential gene deletion/disruption or simultaneous gene targeting (multiplexing)) (54).

In addition to applying CRISPR-Cas9 gene editing to *V. inaequalis*, we have developed a high-throughput screening protocol based on an HRM curve analysis for the identification of CRISPR-Cas9-generated mutants of this fungus with as little as one bp insertion or deletion. We have observed that this highly sensitive method can detect mutant DNA even when mixed in a 5:95 mutant:wt ratio, making it an excellent method for high-throughput screening, as mutants do not need to be single-spore purified prior to screening. This method will be of great value for the identification of mutants generated by CRISPR-Cas9 technology in different fungal species where the mutation efficiency is low.

Methods

Strains used and growth conditions

405 *V. inaequalis* isolate MNH120 from New Zealand (ICMP 13258; (55)) was used for CRISPR-Cas9
406 experiments, and was grown on a cellophane membrane (Waugh Rubber Bands) overlaying
407 PDA (Scharlab) at 22°C with a 16 h light/dark cycle. For long-term storage, *V. inaequalis*
408 cellophane membranes were air-dried overnight and stored at –20°C. *Escherichia coli* strain
409 DH5α (Thermo Fisher Scientific) was used for cloning, propagation and maintenance of
410 Cas9HygAMA-*sgRNA* plasmids, and *E. coli* strain TG1 (kindly provided by Jasna Rakonjac,
411 Massey University) for propagation of the Cas9HygAMAccdB plasmid, in lysogeny broth (LB)
412 at 37°C and 180 rpm, or on LB agar at 37°C.

413

414 **Construction of the Cas9HygAMAccdB plasmid**

415 The ANEp8_Cas9_LIC1 plasmid (35) was kindly provided by Concordia University and was
416 adapted to contain a hygromycin cassette in place of the *pyrG* gene for selection. The 15.6-
417 Kb ANEp8_Cas9_LIC1 plasmid was initially digested with the *Not*I restriction enzyme (New
418 England Biolabs) to liberate a 5.3-Kb fragment containing the AMA1 cassette (purified by gel
419 extraction using an Invitrogen PureLink Quick Gel Extraction Kit) and a 10.3-Kb fragment
420 (purified by gel extraction) containing the *Cas9* and *pyrG* genes. Subsequent digestion of the
421 10.3-Kb fragment with the *Kpn*I restriction enzyme (New England Biolabs) liberated a 9-Kb
422 Cas9 cassette (purified by gel extraction) containing the *Cas9* gene and removal of *pyrG*. To
423 amplify the hygromycin resistance cassette, PCR was performed on the plasmid pDONR221-
424 Hyg (56) with the restriction enzyme-adapted primers KpnI TrpC Hyg DONR R and NotI PgpdA
425 Hyg pDONR F (Table 2), and the resulting product was digested with *Kpn*I and *Not*I prior to
426 ligation. The Cas9 (*Not*I/*Kpn*I-digested) cassette and the hygromycin resistance (*Not*I/*Kpn*I-
427 digested) cassette were ligated with T4 ligase (Invitrogen) at 16°C overnight, creating the

Cas9Hyg plasmid. The Cas9Hyg plasmid was re-digested with *Not*I and treated with alkaline phosphatase (purified by gel extraction) before its T4 ligation with the AMA1 (*Not*I-digested) cassette, creating the Cas9HygAMA plasmid. Modification to the sgRNA protospacer was achieved through ligation-independent cloning (LIC) (35). A mock sgRNA protospacer, containing two *Sap*I restriction enzyme sites, was cloned into the Cas9HygAMA plasmid, creating the Cas9HygAMASapI plasmid, and thus removing the need for the use of LIC with future protospacers. The primers required for the *Sap*I insertion using the LIC method were SapI site CRISPR Fw P1, SapI site CRISPR Rev P1, Fw LIC2 and Rev LIC2 (Table 2). A ccdB lethal cassette was cloned between the two *Sap*I (New England Biolabs) sites to aid in the efficiency of future protospacer cloning. To amplify the ccdB lethal cassette sequence (2 Kb), PCR was performed on the split marker vector pDONR-SM1 (57) with the *Sap*I restriction enzyme-adapted primers SapI ccdB F and SapI ccdB R (Table 2). The resulting product was digested with *Sap*I prior to its ligation with Cas9HygAMASapI (*Sap*I-digested), creating the Cas9HygAMAccdB plasmid.

Protospacer design and cloning

The *V. inaequalis THN* gene was screened for CRISPR-Cas9 target sites with the PAM (NGG) sequence using Geneious v.9.0.5 software (58). Two protospacer sequences targeting the first and second exon of the *THN* gene, respectively, with the best on-target and off-target scores were selected. The selected protospacers were predicted to have no off-target binding sites in the *V. inaequalis* MNH120 PacBio reference genome (unpublished, The New Zealand Institute for Plant and Food Research Limited) using BLASTn. Each protospacer, with the appropriate *Sap*I overhang for Golden Gate cloning into the destination plasmid

Cas9HygAMAccdB, was ordered as a forward and reverse oligonucleotide from Integrated DNA Technologies. The protospacer #20 was generated by pre-annealing 40 ng of the forward (MR135) and reverse (MR136) oligonucleotides (Table 2), and protospacer #4 by pre-annealing 40 ng of the forward (MR137) and reverse (MR138) oligonucleotides (Table 2), in annealing buffer (10 mM Tris-HCl pH 8, 50 mM NaCl, 1 mM EDTA, pH 8) with the following thermocycler program: 5 min at 95°C, 20 sec at 92°C, followed by a decrease of 0.5°C each cycle for 140 cycles, and finally, 1 min at 25°C. Pre-annealed oligonucleotides were cloned into the Cas9HygAMAccdB plasmid using Golden Gate in association with the *Sap*I restriction enzyme to generate sgRNA20 and sgRNA4. Golden Gate reactions were performed with the following thermocycler program: 1 min at 37°C, 1 min at 16°C for 30 cycles, followed by 5 min at 55°C and 5 min at 80°C. Transformants positive for each Cas9HygAMA-*sgRNA* plasmid were screened by colony PCR using Taq DNA polymerase (New England Biolabs) with the forward Cas9HygAMAccdB primer (MR139) and reverse sgRNA-specific primer (MR136 or MR138) (Table 2). Colony PCRs were carried out with the standard manufacturer`s protocol. Sequence authenticity of the sgRNAs was confirmed by PCR amplicon sequencing, provided by the Massey Genome Service (Massey University, Palmerston North, New Zealand), using the MR139 forward Cas9HygAMAccdB primer.

V. inaequalis **protoplast preparation and transformation**

Cas9HygAMA-*sgRNA* plasmids were introduced into *V. inaequalis* using a PEG-mediated protoplast transformation protocol. For this purpose, *V. inaequalis* was first grown on cellophane membranes overlaying PDA for 10–14 days. Fungal mycelia on top and inside cellophane membranes were then macerated in 1.5 ml microcentrifuge tubes using plastic

474 micropestles, transferred to a 250 ml Erlenmeyer flask containing 30 ml potato-dextrose
475 broth (PDB) (Difco™), and cultured without shaking in the dark at 22°C for 48 h. After
476 culturing, fungal material was harvested by centrifugation at 2,800 *g* for 20 min, washed three
477 times with KC buffer (0.60 M KCl, 50 mM $CaCl_2 \cdot 2H_20$), with collection by centrifugation as
478 above after each wash, and incubated in a 250 ml Erlenmeyer flask containing 10 g/L
479 *Trichoderma harzianum* lysing enzymes (Sigma-Aldrich) in 50 mL KC buffer at 24°C and 80 rpm
480 for 4-5 h. Finally, protoplasts were filtered through glass wool, and washed three times with
481 KC buffer as above. Protoplasts were counted using a haemocytometer and re-suspended to
482 a final concentration of 10^4–10^5 protoplasts/ml.

483 Transformation was performed by mixing 100 µl of *V. inaequalis* protoplasts (10^4-10^5
484 protoplasts/ml) with 100 µl of 25% PEG4000, 10 µg of circular Cas9HygAMA-*sgRNA* plasmid
485 DNA, and 5 µl of 50 µM sterile spermidine. The protoplast-PEG mixture was then chilled on
486 ice for 20 min and 500 µl of 25% PEG4000 gently added. Each protoplast-PEG mixture was
487 plated across five Sucrose Hepes (SH) plates (0.6 M sucrose, 5 mM HEPES, 0.6% agar) and
488 incubated at 20°C for 48 h. After incubation, protoplasts were overlaid with ½-strength PDA
489 cooled-down to ~50°C and supplemented with 50 mg/ml hygromycin B (Merck).
490 Transformants appearing on the PDA surface, between two and three weeks after
491 transformation, were transferred to 16-well PDA plates supplemented with 50 mg/ml
492 hygromycin B, and grown until abundantly sporulating. After mutant screening, selected
493 transformants were single-spore purified. This was achieved by re-suspending a single colony
494 in 500 µl sterile water and vortexing for 30 sec, with 100 µl streaked onto 4% water agar (WA)
495 plates and the conidia germinated for 24 h. Following germination, one single germinated
496 conidium was transferred to a cellophane membrane overlaying PDA for continued growth.
497

498 ***V. inaequalis* genomic DNA extraction**

499 Two-to-four week-old cultures of *V. inaequalis* grown on cellophane membranes were freeze-
500 dried and ground to a fine powder in liquid nitrogen with a pre-cooled mortar and pestle, and
501 approximately 300 mg of powder was transferred to a 1.5 ml microcentrifuge tube. To this, 1
502 ml of DNA extraction buffer (0.5 M NaCl, 10 mM Tris-HCl, 10 mM EDTA, 1% SDS, pH 7.5) was
503 added, vortexed, and incubated at 65°C for 30 min, followed by 2 min incubation at room
504 temperature (RT). Fungal material was collected by centrifugation at 16,000 *g* for 2 min and
505 800 µl of supernatant was transferred to a fresh 1.5 ml microcentrifuge tube. Then, 4 µl of
506 RNase A (20 mg/ml) (Invitrogen) was added and samples were incubated at 37°C for 15 min.
507 After incubation, a 0.5 volume of phenol and a 0.5 volume of chloroform:isoamyl alcohol
508 (24:1) were added and samples were centrifuged for 5 min at 16,000 *g*. The aqueous phase
509 was then transferred to a fresh 1.5 ml microcentrifuge tube and 1 volume of
510 phenol:chloroform (1:1) was added. Samples were again centrifuged at 16,000 *g* for 5 min
511 and the supernatant transferred to a new 1.5 ml microcentrifuge tube. The
512 chloroform:isoamyl alcohol (24:1) step was then repeated and the supernatant was
513 transferred to a new 1.5 ml microcentrifuge tube. Genomic DNA was precipitated by the
514 addition of a 0.1 volume of 3 M sodium acetate (pH 5.2) and two volumes of 95% ethanol.
515 Samples were mixed by inversion and incubated overnight at –20°C. Following incubation, the
516 precipitated DNA was collected by centrifugation at 16,000 *g* for 30 min, and the supernatant
517 was decanted. The genomic DNA pellet was then washed with 200 µl of 70% ethanol and
518 collected by centrifugation at 16,000 *g* for 5 min. Finally, the genomic DNA pellet was air-
519 dried for 15-30 min and suspended in 50 µl of MilliQ water.

520

High resolution melting curve analysis

A positive control for the HRM curve analysis was created by site-directed mutagenesis. First, primers MR161 and MR162 (Table 2) were phosphorylated with T4 Polynucleotide Kinase (New England Biolabs) at 37°C for 1 h in a 4.5 µl reaction volume with 10 µM primer, 10x T4 ligase buffer (New England Biolabs) and 0.4 µl of T4 polynucleotide kinase (New England Biolabs). The *THN* gene was amplified with the phosphorylated primers MR161-MR162 using Phusion Flash High-Fidelity PCR Master Mix (Thermo Fisher Scientific) and purified using an OMEGA Gel Extraction kit. The pICH41021 plasmid was digested with the *Sma*I restriction enzyme in a 50 µl volume for 2 h at 37°C. Digested plasmid was then de-phosphorylated with Shrimp Alkaline Phosphatase (rSAP) (New England Biolabs) for 30 min at 37°C, with the reaction subsequently heat-inactivated at 65°C for 5 min. Finally, the *THN* gene was ligated to pICH41021 in a 3:1 molar ratio using T4 Ligase (New England Biolabs) at 4°C overnight and transformed by heat shock into chemically competent *E. coli* cells. Positive transformants were confirmed by colony PCR. Next, the pICH41021-*THN* plasmid was amplified with overlapping primers MR182 and MR183 to introduce a mutation in the *THN* gene that substituted a thymine and cytosine at nucleotide positions 26 and 27 for two guanines. The resulting re-circularized pICH41021-$THN_{TC(26/27)GG}$ plasmid was confirmed by sequencing.

Two sets of primers (MR170-MR171 and MR172-MR173) were designed with Geneious v.9.0.5 software for use in the HRM curve analysis (Table 2). These primers were designed to amplify the DNA region in the *THN* gene recognized by the sgRNA (and thus, edited by the Cas9 endonuclease), with an amplicon size of 123 bp (MR172-MR173) and 230 bp (MR170-MR171). Primers were tested to be specific and suitable for HRM by performing

543 an HRM curve analysis with DNA standards (wt and engineered positive control), as described
544 below, with the resulting amplicons resolved by electrophoresis on a 1.5% TAE gel.

545 The HRM curve analysis was performed using a LightCycler 480 Instrument (Roche)
546 with the AccuMelt HRM SuperMix fluorescent dye (DNAture) in a 20 µL reaction with 1x
547 AccuMelt HRM SuperMix, 300 nM forward primers (MR172), 300 nM reverse primer (MR173)
548 and 1.5 ng of genomic DNA template or 0.01 ng of the puc19-THN$_{TC(26/27)GG}$ plasmid. At least
549 two technical replicates were performed for each sample. The qPCR amplification was
550 performed with the following program: initial denaturation of 5 min at 95°C, followed by 40
551 cycles of 95°C for 8 sec, 60°C for 15 sec, 70°C for 20 sec, with one fluorescence reading per
552 annealing step. The qPCR was followed by a melting program consisting of 95°C for 1 min,
553 40°C for 1 min, 76°C for 1 sec, and then a continuous 92°C with 25 acquisitions per degree
554 followed by a cooling step of 40°C for 30 sec. The HRM curve data were analysed with the
555 LightCycler 480 gene scanning software. To confirm mutants identified by HRM, the *THN* gene
556 was amplified with Phusion Flash High-Fidelity PCR Master Mix using primers MR161 and
557 MR162, with the resultant PCR amplicons gel-purified as above and sequenced using primer
558 MR161.

559

560 **Ethics approval and consent to participate**

561 Not applicable.

562 **Availability of data and materials**

563 No substantive datasets were generated during the course of this study and all data are
564 presented within.

Competing interests

The authors declare that they have no competing interests.

Funding

MRF and CHM are supported by the Marsden Fund Council from Government funding (project ID 17-MAU-100), managed by Royal Society Te Apārangi. SA and JKB received funding from The New Zealand Institute for Plant and Food Research Limited, Strategic Science Investment Fund, Project number: 12070. DH, JS, RDJ and LJJ are supported by the MBIE partnership programme: Novel variation for a persistent problem (project ID C10X1902). AgResearch work was also supported through a QEII technicians' study award (to JS) and the New Zealand Strategic Science Investment Fund (SSIF) contract A20067.

Author contributions

MR, JKB, KMP, REB, RDJ, LJJ and CHM conceived the project. MR, SA, DH and JS performed the research. All authors contributed to the writing and reviewing of the manuscript.

Acknowledgements

We thank Professor Adrian Tsang (Center for Functional and Structural Genomics Biology, Concordia University, Canada) for hosting JS and providing the original CRISPR-Cas9 vectors. We also thank Natasha Forester and Pranav Chettri for useful discussions around vector modification.

References

1. Bowen JK, Mesarich CH, Bus VG, Beresford RM, Plummer KM, Templeton MD. *Venturia inaequalis*: the causal agent of apple scab. *Molecular Plant Pathology*. 2011;12(2):105-22.

2. Le Cam B, Sargent D, Gouzy J, Amselem J, Bellanger M-N, Bouchez O, et al. Population genome gequencing of the scab fungal species *Venturia inaequalis*, *Venturia pirina*, *Venturia aucupariae* and *Venturia asperata*. *G3: Genes, Genomes, Genetics*. 2019;9(8):2405-14.

3. González-Domínguez E, Armengol J, Rossi V. Biology and epidemiology of *Venturia* species affecting fruit crops: A Review. *Frontiers in Plant Science*. 2017;8(1496).

4. Jha G, Thakur K, Thakur P. The *Venturia* apple pathosystem: pathogenicity mechanisms and plant defense responses. *Journal of Biomedicine and Biotechnology*. 2009;2009:680160.

5. Deng CH, Plummer KM, Jones DAB, Mesarich CH, Shiller J, Taranto AP, et al. Comparative analysis of the predicted secretomes of Rosaceae scab pathogens *Venturia inaequalis* and *V. pirina* reveals expanded effector families and putative determinants of host range. *BMC Genomics*. 2017;18(1):339.

6. Lichtner FJ, Jurick WM, Ayer KM, Gaskins VL, Villani SM, Cox KD. A genome resource for several North American *Venturia inaequalis* isolates with multiple fungicide resistance phenotypes. *Phytopathology*. 2020;110(3):544-6.

7. Papp D, Singh J, Gadoury D, Khan A. New North American isolates of *Venturia inaequalis* can overcome apple scab resistance of *Malus floribunda* 821. *Plant Disease*. 2020;104(3):649-55.

609 8. Passey TAJ, Armitage AD, Xu X. Annotated draft genome sequence of the apple scab
610 pathogen *Venturia inaequalis*. *Microbiology Resource Announcements*.
611 2018;7(12):e01062-18.
612 9. Passey TAJ, Armitage AD, Sobczyk MK, Shaw MW, Xu X. Genomic sequencing indicates
613 non-random mating of *Venturia inaequalis* in a mixed cultivar orchard. *Plant*
614 *Pathology*. 2020;69(4):669-76.
615 10. Fitzgerald AM, Mudge AM, Gleave AP, Plummer KM. *Agrobacterium* and PEG-
616 mediated transformation of the phytopathogen *Venturia inaequalis*. *Mycological*
617 *Research*. 2003;107(7):803-10.
618 11. Bowen JK, Mesarich CH, Rees-George J, Cui W, Fitzgerald A, Win J, et al. Candidate
619 effector gene identification in the ascomycete fungal phytopathogen *Venturia*
620 *inaequalis* by expressed sequence tag analysis. *Molecular Plant Pathology*.
621 2009;10(3):431-48.
622 12. Kucheryava N, Bowen JK, Sutherland PW, Conolly JJ, Mesarich CH, Rikkerink EH, et al.
623 Two novel *Venturia inaequalis* genes induced upon morphogenetic differentiation
624 during infection and *in vitro* growth on cellophane. *Fungal Genetics and Biology*.
625 2008;45(10):1329-39.
626 13. Mesarich CH, Schmitz M, Tremouilhac P, McGillivray DJ, Templeton MD, Dingley AJ.
627 Structure, dynamics and domain organization of the repeat protein Cin1 from the
628 apple scab fungus. *Biochimica Biophysica Acta Proteins and Proteomics*.
629 2012;1824(10):1118-28.
630 14. Shiller J, Van de Wouw AP, Taranto AP, Bowen JK, Dubois D, Robinson A, et al. A large
631 family of *AvrLm6-like* genes in the apple and pear scab pathogens, *Venturia inaequalis*
632 and *Venturia pirina*. *Frontiers in Plant Science*. 2015;6(980).

15. Feurtey A, Guitton E, De Gracia Coquerel M, Duvaux L, Shiller J, Bellanger M-N, et al. Threat to Asian wild apple trees posed by gene flow from domesticated apple trees and their "pestified" pathogens. *Molecular Ecology*. 2020;29(24):4925-41.

16. Fitzgerald A, Van Kan JA, Plummer KM. Simultaneous silencing of multiple genes in the apple scab fungus, *Venturia inaequalis*, by expression of RNA with chimeric inverted repeats. *Fungal Genetics and Biology*. 2004;41(10):963-71.

17. Salame TM, Ziv C, Hadar Y, Yarden O. RNAi as a potential tool for biotechnological applications in fungi. *Applied Microbiology and Biotechnology*. 2011;89(3):501-12.

18. Nakayashiki H, Nguyen QB. RNA interference: roles in fungal biology. *Current Opinion in Microbiology*. 2008;11(6):494-502.

19. Doudna JA, Charpentier E. The new frontier of genome engineering with CRISPR-Cas9. *Science*. 2014;346(6213):1258096.

20. Schuster M, Kahmann R. CRISPR-Cas9 genome editing approaches in filamentous fungi and oomycetes. *Fungal Genetics and Biology*. 2019;130:43-53.

21. Fang Y, Tyler BM. Efficient disruption and replacement of an effector gene in the oomycete *Phytophthora sojae* using CRISPR/Cas9. *Molecular Plant Pathology*. 2016;17(1):127-39.

22. Foster AJ, Martin-Urdiroz M, Yan X, Wright HS, Soanes DM, Talbot NJ. CRISPR-Cas9 ribonucleoprotein-mediated co-editing and counterselection in the rice blast fungus. *Scientific Reports*. 2018;8(1):14355.

23. Schuster M, Schweizer G, Reissmann S, Kahmann R. Genome editing in *Ustilago maydis* using the CRISPR–Cas system. *Fungal Genetics and Biology*. 2016;89:3-9.

24. Idnurm A, Urquhart AS, Vummadi DR, Chang S, Van de Wouw AP, López-Ruiz FJ. Spontaneous and CRISPR/Cas9-induced mutation of the osmosensor histidine kinase

of the canola pathogen *Leptosphaeria maculans*. *Fungal Biology and Biotechnology*. 2017;4:12.

25. Sander JD, Joung JK. CRISPR-Cas systems for editing, regulating and targeting genomes. *Nature Biotechnology*. 2014;32(4):347-55.

26. Krappmann S. Gene targeting in filamentous fungi: the benefits of impaired repair. *Fungal Biology Reviews*. 2007;21(1):25-9.

27. Vouillot L, Thélie A, Pollet N. Comparison of T7E1 and surveyor mismatch cleavage assays to detect mutations triggered by engineered nucleases. *G3: Genes, Genomes, Genetics*. 2015;5(3):407-15.

28. Zhu X, Xu Y, Yu S, Lu L, Ding M, Cheng J, et al. An efficient genotyping method for genome-modified animals and human cells generated with CRISPR/Cas9 system. *Scientific Reports*. 2014;4(1):6420.

29. Denbow CJ, Lapins S, Dietz N, Scherer R, Nimchuk ZL, Okumoto S. Gateway-compatible CRISPR-Cas9 vectors and a rapid detection by high-resolution melting curve analysis. *Frontiers in Plant Science*. 2017;8(1171).

30. Reed GH, Wittwer CT. Sensitivity and specificity of single-nucleotide polymorphism scanning by high-resolution melting analysis. *Clinical Chemistry*. 2004;50(10):1748-54.

31. Simko I. High-resolution DNA melting analysis in plant research. *Trends in Plant Science*. 2016;21(6):528-37.

32. Wittwer CT. High-resolution DNA melting analysis: advancements and limitations. *Human Mutation*. 2009;30(6):857-9.

33. Dufresne SD, Belloni DR, Wells WA, Tsongalis GJ. *BRCA1* and *BRCA2* mutation screening using SmartCycler II high-resolution melt curve analysis. A*rchives of Pathology & Laboratory Medicine*. 2006;130(2):185-7.

681 34. Li R, Ba Y, Song Y, Cui J, Zhang X, Zhang D, et al. Rapid and sensitive screening and
682 identification of CRISPR/Cas9 edited rice plants using quantitative real-time PCR
683 coupled with high resolution melting analysis. *Food Control*. 2020;112:107088.
684 35. Song L, Ouedraogo J-P, Kolbusz M, Nguyen TTM, Tsang A. Efficient genome editing
685 using tRNA promoter-driven CRISPR/Cas9 gRNA in *Aspergillus niger*. *PLoS One*.
686 2018;13(8):e0202868-e.
687 36. Aleksenko A, Clutterbuck AJ. Autonomous plasmid replication in *Aspergillus nidulans*:
688 AMA1 and MATE Elements. *Fungal Genetics and Biology*. 1997;21(3):373-87.
689 37. Nødvig CS, Nielsen JB, Kogle ME, Mortensen UH. A CRISPR-Cas9 system for genetic
690 engineering of filamentous fungi. *PLoS One*. 2015;10(7):e0133085.
691 38. Doench JG, Hartenian E, Graham DB, Tothova Z, Hegde M, Smith I, et al. Rational
692 design of highly active sgRNAs for CRISPR-Cas9–mediated gene inactivation. *Nature*
693 *Biotechnology*. 2014;32(12):1262-7.
694 39. Hamada W, Reignault P, Bompeix G, Boccara M. Transformation of *Botrytis cinerea*
695 with the hygromycin B resistance gene, *hph*. *Current Genetics*. 1994;26(3):251-5.
696 40. Sánchez-Torres P, González R, Pérez-González JA, González-Candelas L, Ramón D.
697 Development of a transformation system for *Trichoderma longibrachiatum* and its use
698 for constructing multicopy transformants for the *egl1* gene. *Applied Microbiology and*
699 *Biotechnology*. 1994;41(4):440-6.
700 41. DiCarlo JE, Norville JE, Mali P, Rios X, Aach J, Church GM. Genome engineering in
701 *Saccharomyces cerevisiae* using CRISPR-Cas systems. *Nucleic Acids Research*.
702 2013;41(7):4336-43.

703 42. Khan H, McDonald MC, Williams SJ, Solomon PS. Assessing the efficacy of CRISPR/Cas9
704 genome editing in the wheat pathogen *Parastagonspora nodorum*. *Fungal Biology and*
705 *Biotechnology*. 2020;7(1):4.
706 43. Shi TQ, Liu GN, Ji RY, Shi K, Song P, Ren LJ, et al. CRISPR/Cas9-based genome editing of
707 the filamentous fungi: the state of the art. *Applied Microbiology and Biotechnology*.
708 2017;101(20):7435-43.
709 44. Nødvig CS, Hoof JB, Kogle ME, Jarczynska ZD, Lehmbeck J, Klitgaard DK, et al. Efficient
710 oligo nucleotide mediated CRISPR-Cas9 gene editing in Aspergilli. *Fungal Genetics and*
711 *Biology*. 2018;115:78-89.
712 45. Słomka M, Sobalska-Kwapis M, Wachulec M, Bartosz G, Strapagiel D. High Resolution
713 Melting (HRM) for high-throughput genotyping—Limitations and caveats in practical
714 case studies. *International Journal of Molecular Sciences*. 2017;18(11):2316.
715 46. Morgens DW, Wainberg M, Boyle EA, Ursu O, Araya CL, Tsui CK, et al. Genome-scale
716 measurement of off-target activity using Cas9 toxicity in high-throughput screens.
717 *Nature Communications*. 2017;8(1):15178.
718 47. Al Abdallah Q, Souza ACO, Martin-Vicente A, Ge W, Fortwendel JR. Whole-genome
719 sequencing reveals highly specific gene targeting by in vitro assembled Cas9-
720 ribonucleoprotein complexes in *Aspergillus fumigatus*. *Fungal Biology and*
721 *Biotechnology*. 2018;5(1):11.
722 48. Chen C, Bock CH, Wood BW. Draft genome sequence of *Venturia carpophila*, the
723 causal agent of peach scab. *Standards in Genomic Sciences*. 2017;12:68.
724 49. Cooke IR, Jones D, Bowen JK, Deng C, Faou P, Hall NE, et al. Proteogenomic analysis of
725 the *Venturia pirina* (Pear Scab Fungus) secretome reveals potential effectors. *Journal*
726 *of Proteome Research*. 2014;13(8):3635-44.

50. Jaber MY, Bao J, Gao X, Zhang L, He D, Wang X, et al. Genome sequence of *Venturia oleaginea*, the causal agent of olive leaf scab. *Molecular Plant-Microbe Interactions*. 2020;33(9):1095-7.

51. Johnson S, Jones D, Thrimawithana AH, Deng CH, Bowen JK, Mesarich CH, et al. Whole genome sequence resource of the Asian pear scab pathogen *Venturia nashicola*. *Molecular Plant-Microbe Interactions*. 2019;32(11):1463-7.

52. Winter DJ, Charlton ND, Krom N, Shiller J, Bock CH, Cox MP, et al. Chromosome-Level reference genome of *Venturia effusa*, causative agent of pecan scab. *Molecular Plant-Microbe Interactions*. 2020;33(2):149-52.

53. Prokchorchik M, Won K, Lee Y, Choi ED, Segonzac C, Sohn KH. High contiguity whole genome sequence and gene annotation resource for two *Venturia nashicola* isolates. *Molecular Plant-Microbe Interactions*. 2019;32(9):1091-4.

54. Schuster M, Schweizer G, Kahmann R. Comparative analyses of secreted proteins in plant pathogenic smut fungi and related basidiomycetes. *Fungal Genetics and Biology*. 2018;112:21-30.

55. Stehmann C, Pennycook S, Plummer KM. Molecular identification of a sexual interloper: the pear pathogen, *Venturia pirina*, has sex on apple. *Phytopathology*. 2001;91(7):633-41.

56. Fleetwood DJ, Scott B, Lane GA, Tanaka A, Johnson RD. A complex ergovaline gene cluster in *Epichloë* endophytes of grasses. *Applied and Environmental Microbiology*. 2007;73(8):2571.

57. Rahnama M, Forester N, Ariyawansa KGSU, Voisey CR, Johnson LJ, Johnson RD, et al. Efficient targeted mutagenesis in *Epichloë festucae* using a split marker system. *Journal of Microbiological Methods*. 2017;134:62-5.

751 58. Kearse M, Moir R, Wilson A, Stones-Havas S, Cheung M, Sturrock S, et al. Geneious
752 Basic: an integrated and extendable desktop software platform for the organization
753 and analysis of sequence data. *Bioinformatics*. 2012;28(12):1647-9.

754